Effects of Stochastic Single-Molecule Reactions on Coherent Ensemble Oscillations in the KaiABC Circadian Clock

Masaki Sasai
Department of Applied Physics, Nagoya University, Nagoya 464-8603, Japan
email: masakisasai@nagoya-u.jp
telephone +81-52-789-4763

Abstract

How do many constituent molecules in a biochemical system synchronize, giving rise to coherent system-level oscillations? One system that is particularly suitable for use in studying this problem is a mixture solution of three cyanobacterial proteins, KaiA, KaiB, and KaiC: phosphorylation level of KaiC shows stable oscillations with a period of approximately 24 hours when these three Kai proteins are incubated with ATP in vitro. Here, we analyze the mechanism behind synchronization in the KaiABC system theoretically by enhancing a model previously developed by the present author. Our simulation results suggest that positive feedback between stochastic ATP hydrolysis and the allosteric structural transitions in KaiC molecules drives oscillations of individual molecules and promotes synchronization of oscillations of many KaiC molecules. Our simulations also show that ATPase activity of KaiC is correlated with the oscillation frequency of an ensemble of KaiC molecules. These results suggest that stochastic ATP hydrolysis in each KaiC molecule plays an important role in regulating the coherent system-level oscillations. This property is robust against changes in the binding and unbinding rate constants for KaiA to/from KaiC or KaiB, but the oscillations are sensitive to the rate constants of the KaiC phosphorylation and dephosphorylation reactions.

Introduction

Circadian rhythms are biochemical oscillations where the amounts or characteristics of particular molecules vary with approximately 24 hour period. To clarify the mechanism behind such oscillations, we need to understand how oscillations of individual molecules in the system synchronize with each other to give rise to coherent oscillations of a many-molecule ensemble. One way to investigate this synchronization mechanism is to analyze the effects of modifying individual molecules on the synchronization and ensemble-level dynamics. One system that is particularly suitable for use in studying this problem is a mixture solution of three cyanobacterial proteins, KaiA, KaiB, and KaiC: when these three Kai proteins are incubated with ATP in vitro, the phosphorylation level of KaiC shows a stable circadian oscillation.[1] In the present study, we develop a theoretical model of this prototypical circadian oscillator in order to analyze the relationships between reactions in individual molecules and the ensemble dynamics.

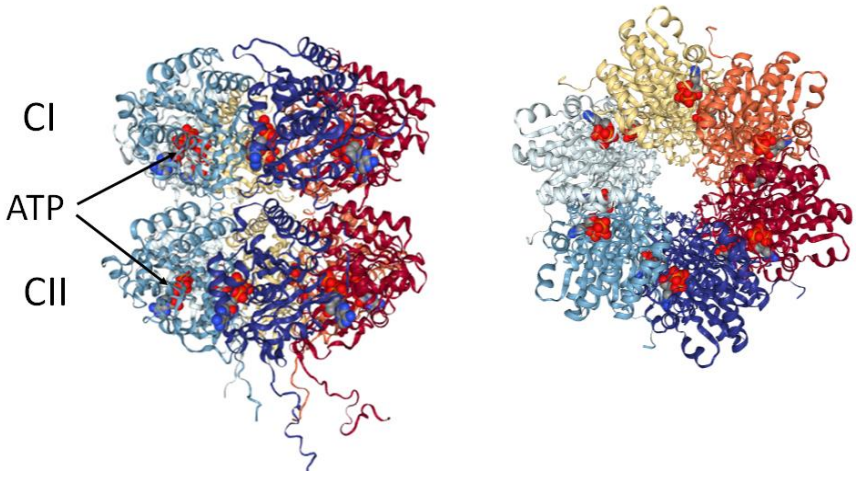

Figure 1. Crystal structure of a KaiC hexamer. Protein Data Bank (PDB) code 2GBL deposited by Pattanayek et al.[11] visualized by using NGL Viewer.[46] Side (left) and top (right) views with different chains rendered in different colors.

The structures and reactions of Kai proteins have been actively investigated.[2, 3] An individual KaiC monomer is composed of tandemly duplicated N-terminal (CI) and C-terminal (CII) domains[4] and six monomers of KaiC assemble into a hexamer[5,6] to form CI and CII rings,[7] as shown in Figure 1. Here, we denote this hexamer by C_6. Two residues in each CII domain, Thr432 and Ser431, amounting to 12 sites in a CII ring, are phosphorylated and dephosphorylated with a period of approximately 24 hours.[8,9]

KaiA forms a dimer[10] (A_2) and binds to a CII ring of KaiC[11] as $A_2 + C_6 \rightleftarrows C_6A_2$, and this C_6A_2 complex promotes phosphorylation (P) of Thr432/Ser431.[12] Recent observations with cryo-electron microscopy (EM),[13] mass spectrometry,[13] and atomic force microscopy (AFM)[14] have shown that KaiB monomers bind to the CI domains of KaiC subunits to form C_6B_i complexes, with $0 \leq i \leq 6$. In addition, KaiA dimers then bind to the KaiB monomers in C_6B_i to form $C_6B_iA_{2j}$, with $0 \leq j \leq i$. The cryo-EM structure of $C_6B_6A_{12}$ is shown in Figure 2. This KaiB binding prevents binding of KaiA

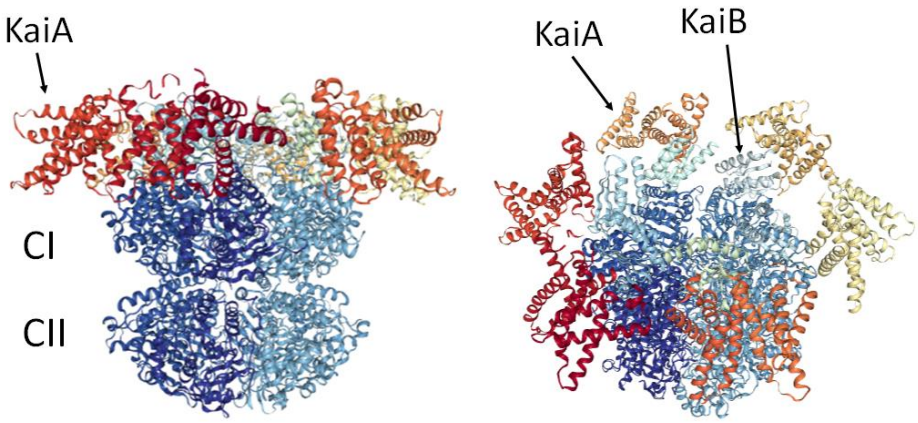

Figure 2. Cryo-EM structure of a KaiCBA complex, $C_6B_6A_{12}$. PDB code 5N8Y deposited by Snijder et al.[13] visualized by using NGL Viewer.[46] Views from two different angles, with different chains rendered in different colors. The C-terminal tails visible in Figure 1 are not shown.

to the CII, promoting the auto-dephosphorylation (dP) of KaiC.[15,16] Thus, when KaiA and KaiB alternately bind to KaiC in this way, alternating P and dP phases appear, yielding oscillatory dynamics.

Many theoretical models have been developed to analyze these P/dP oscillations. In particular, the dynamics of molecular ensembles have been studied using macroscopic models that describe the reactions in terms of kinetic differential equations, representing the concentrations of various molecular species as continuous variables.[8,17-22] Stochastic Monte Carlo-type molecular ensemble simulations have also been used to investigate how the reactions of individual molecules relate to the ensemble-level dynamics.[19,23-27]

Based on these theoretical models, various nonlinear mechanisms have been proposed to explain how the oscillations synchronize. In an earliest theoretical attempt, synchronization was explained by assuming direct KaiC-KaiC interactions through aggregation of KaiC hexamers in solution,[17] but there has been no experimental support

for such aggregation. The other proposed mechanism of KaiC-KaiC interactions is exchange of monomers between KaiC hexamers; exchanging monomers should shuffle differently phosphorylated monomers,[23,28] thereby affecting the P/dP reaction rates in the hexamers. In addition, the exchange frequency depends on the phosphorylation level of KaiC hexamers.[28] In this way, coupling between monomer exchange and P/dP reactions may act as a synchronization mechanism.[17,23-26]

The other proposed mechanisms are based on KaiA sequestration[8,14,18-22,27,29,30]. When KaiA binds to a certain KaiC state and the KaiA concentration is not too large, this KaiA binding (or sequestration) should decrease the concentration of free unbound KaiA in solution, decreasing the rate at which KaiA binds to the other KaiC states. Since binding KaiA to the CII ring is necessary for phosphorylation, decrease in the KaiA binding rate should result decreased phosphorylation rate. This should, in turn, cause "congestion" of the molecules in the P/dP kinetic cycle, leading to the synchronization of many KaiC molecules. Here, several different KaiC states were assumed to be "absorbers" that sequester KaiA; specifically, a highly phosphorylated state of KaiC,[8,22] a lowly phosphorylated state of KaiC in the P-phase,[14,18-20,27] and a KaiCB complex formed in the dP-phase[21,27,29,30] were proposed as possible absorbers.

In this way, a variety of different models were proposed for explaining synchronization and we still do not have a convergent view; monomer exchange and KaiA sequestration are not mutually exclusive, meaning that both of these mechanisms can coexist, and there is currently no experimental evidence that decisively favors one scenario over the other. However, the recent cryo-EM observation has revealed[13] that a KaiCB complex can absorb a maximum of six KaiA dimers to form $C_6B_6A_{12}$. This high KaiA absorption ability should play an important role in synchronization and the mechanism needs to be reconsidered theoretically by taking account of the KaiA sequestration into the KaiCB complex. Therefore, in the present study, we focus on the KaiA sequestration mechanism by developing a quantitative model based on the cryo-EM structure of the KaiCBA complex. Based on assuming KaiA is sequestered into KaiCBA complex, we show that the model reasonably explains the observed synchronization features when ATPase reactions in KaiC are accounted for.

The slow ATPase activity of KaiC is one of its most significant features. Biochemical observations have shown that, for each KaiC subunit, about 10 and 4-6 ATP molecules/day are hydrolyzed in the CI and CII domains, respectively[31,32] Here, an important finding is that the ATPase activity is correlated with the P/dP oscillation frequency: by comparing various KaiC mutants, the ATPase activity measured in the steady state (which does not contain KaiA or KaiB) has been shown to be correlated with

the P/dP oscillation frequency measured in the presence of KaiA and KaiB.[31,32]

Based on this observation, it has been hypothesized that the structural changes in KaiC induced by the slow ATPase reaction act as a pacemaker of the circadian oscillation in the Kai system.[31,33] It has also been shown that the ATPase activity in hexamer rings of truncated CI domains is correlated with the oscillation frequency of full-length KaiC.[32] Since the ATP binding site in the CII domain is located near Thr432 and Ser431, it is natural to assume that a phosphate group generated by the ATP hydrolysis in CII is involved in Thr432 or Ser431 phosphorylation. Given that, it seems rather obvious that the ATPase activity in CII is correlated with the P/dP rhythm. However, it is far from evident why the ATPase activity in CI is correlated with the P/dP cycle in CII at the ensemble level. Therefore, clarifying the mechanism behind this correlation is one of the keys to understanding the relationship between the reaction dynamics in individual molecules and the ensemble-level P/dP dynamics. The roles played by ATPase reactions in KaiC have only recently been analyzed theoretically,[27,29,30] so further comprehensive studies of the ATPase reactions are needed.

In the present paper, we enhance the multifold feedback model that we previously developed to analyze the effects of ATPase reactions.[29,30] This model assumes multiple feedback relationships among the reactions and allosteric structural changes in KaiC. The previous version of the model assumed that both the KaiA and KaiB (un)binding reactions obey slow kinetics with low association and dissociation rates. Indeed, there are experimental evidences to suggest that the rates of KaiB binding/unbinding are much smaller than those of typical protein association/dissociation reactions.[21,34] However, the recent AFM measurements revealed that the timescale of KaiA binding/unbinding is of the order of seconds,[14] which is much shorter than the timescale of KaiB binding/unbinding.

Given these new results, the present paper adjusts our multifold feedback model to take account of the observed rapid KaiA binding/unbinding reactions and thereby investigate the effects of ATPase reactions on the ensemble-level dynamics. Based on this improved model, we show that the ATPase reactions are needed to synchronize many molecules. By simulating this model numerically, we investigate the physical mechanisms by which ATPase reactions in the CI domains drive individual oscillations and promote synchronization.

Theoretical Methods

Our multifold feedback model is based on the following four major assumptions: (1) Binding/unbinding and ATP hydrolysis reactions are regulated by the allosteric structure

changes in KaiC. (2) Direct interactions between different KaiC molecules do not play a significant role, but indirect interactions via KaiA sequestration are important. (3) Binding/unbinding and ATP hydrolysis reactions affect the allosteric structure changes. This, combined with the assumption 1, defines the multifold feedback relationships among the reactions and structure changes. (4) ATP hydrolysis takes place stochastically in each CI domain of individual KaiC molecules. In this section, we explain each of these assumptions in turn. Major difference between the present and previous versions of the model is the assumption that KaiA binding/unbinding is much faster than the other reactions, including the KaiB binding/unbinding, P/dP, and ATP hydrolysis reactions. The new model therefore treats KaiA binding/unbinding using the quasi-equilibrium approximation (see Eqs. 2, 3, and 6 below). We also discuss the effects of modifying the other reaction rates in the Results and Discussion section.

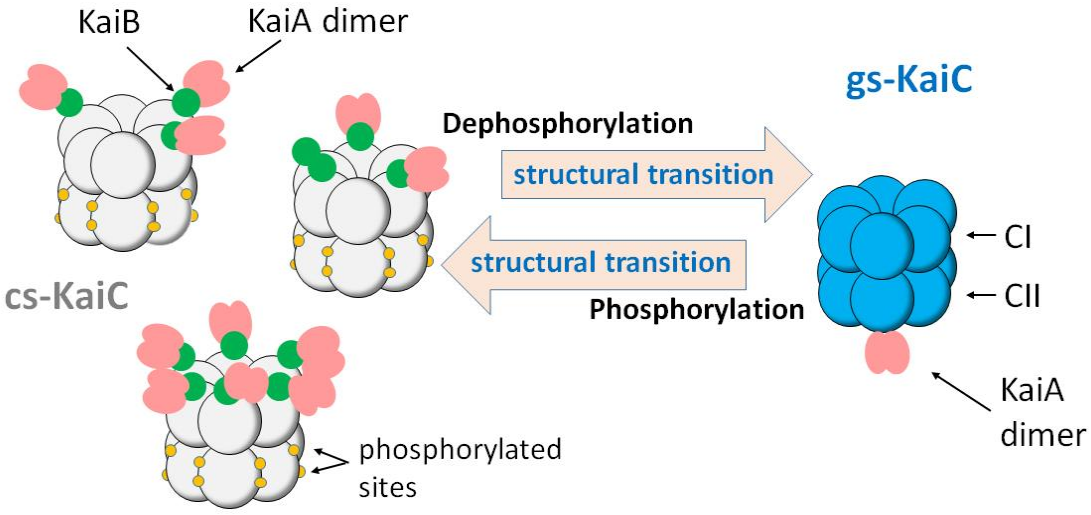

Figure 3. Coordinated dynamics of KaiC hexamers. The phosphorylation and dephosphorylation reactions, binding of KaiA dimer (pink) to the CII ring, binding of KaiB monomers (green) to the CI domains of hexamer subunits are coordinated by allosteric structure changes between two states; competent state (cs, gray) and ground state (gs, blue). Variously different stoichiometries are possible in the KaiCBA complex (left).

Reactions regulated by allosteric structure changes. The P/dP rhythm is associated with cyclical changes in binding affinities of KaiA and KaiB to KaiC. As shown in Figure 3, our multifold feedback model assumes that these binding affinity changes are due to allosteric communication between CI and CII domains: when CI is in a structural state with a higher binding affinity to KaiB, the CII structure tends to have a lower binding affinity to KaiA, and when the CII structure has a higher binding affinity to KaiA, the CI structure tends to have a lower binding affinity to KaiB. Indeed, small-angle X-ray scattering,[35] NMR spectroscopy,[36,37] and biochemical analysis[38] have shown that KaiC hexamers have different structures during the P and dP phases. Oyama et al. referred to the structural state in the P phase as ground state (gs) and that in the dP phase as competent state (cs). cs-KaiC can dissociate into monomers, so that cs-KaiC is less stable than gs-KaiC.[38] Therefore, we can consider that KaiA binds to the CII ring in gs-KaiC, while KaiB binds to the CI domains in cs-KaiC, and that the allosteric transitions between the gs and cs regulate the binding affinities of KaiA and KaiB to KaiC. Here, we write the structural state of the *k*th KaiC hexamer at time *t* as $W(k,t)$, where $W(k,t)=1$ for gs-KaiC and $W(k,t)=-1$ for cs-KaiC. Thus, the model describes the allosteric transitions between the gs and cs in terms of dynamical changes in the range $-1 \leq W(k,t) \leq 1$.

We describe the dependence of binding affinities on the structure by defining binding and unbinding rate constants for the *k*th KaiC hexamer at time *t* in terms of $W(k,t)$:

$$\begin{aligned} h_A(k,t) &= h_{A0}[1+\tanh(W(k,t)/A_W)], \\ f_A(k,t) &= f_{A0}[1-\tanh(W(k,t)/A_W)], \\ h_B(k,t) &= h_{B0}[1-\tanh(W(k,t)/B_W)], \\ f_B(k,t) &= f_{B0}[1+\tanh(W(k,t)/B_W)], \end{aligned} \qquad (1)$$

where $h_A(k,t)$ and $f_A(k,t)$ are the binding and unbinding rate constants of KaiA to/from the CII ring, respectively, and $h_B(k,t)$ and $f_B(k,t)$ are the binding and unbinding rate constants of KaiB to/from the CI domains, respectively. A_W and B_W are constants to determine the dependence of the rate constants on the structure and h_{A0}, f_{A0}, h_{B0}, and f_{B0} are constants to set the timescale of binding/unbinding reactions. Eq. 1 assumes that KaiA binds to the CII rings preferentially in gs-KaiC ($W(k,t) \approx 1$) and KaiB binds to the CI domains preferentially in cs-KaiC ($W(k,t) \approx -1$).

There are multiple protein complexes, $\mathrm{C_6A_2}$, $\mathrm{C_6}$, and $\mathrm{C_6B_iA_{2j}}$, coexisting in the system. We write the probabilities of the *k*th KaiC hexamer forming $\mathrm{C_6A_2}$, $\mathrm{C_6}$, and $\mathrm{C_6B_iA_{2j}}$ complexes at time *t* as $P_{\mathrm{C_6A_2}}(k,t)$, $P_{\mathrm{C_6B_0}}(k,t)$, and $P_{\mathrm{C_6B_iA_{2j}}}(k,t)$,

respectively, where C_6 is represented as C_6B_0. The kinetic equation for binding and unbinding reactions of KaiA to the CII rings is $\frac{d}{dt}P_{C_6A_2}(k,t) = h_A x P_{C_6B_0}(k,t) - f_A P_{C_6A_2}(k,t)$, where x is the concentration of free unbound KaiA dimers. Here, we assume that most of KaiA molecules exist as dimers, because no experiments have yet found isolated KaiA monomers in solution under oscillatory conditions. Because binding and unbinding reactions of KaiA are so much faster than KaiB or P/dP reactions, we can approximate the KaiA binding/unbinding as a quasi-equilibrium. Therefore, by setting $\frac{d}{dt}P_{C_6A_2}(k,t) = 0$, we have

$$P_{C_6A_2}(k,t) = x g_A(k,t) P_{C_6B_0}(k,t), \qquad (2)$$

where $g_A(k,t) = h_A(k,t)/f_A(k,t)$ is the association constant. By writing $P_{C_6B_i}(k,t) = \sum_{j=0}^{i} P_{C_6B_iA_{2j}}(k,t)$, the binding and unbinding reactions of KaiB to/from the CI are described by

$$\begin{aligned}
\frac{d}{dt}P_{C_6B_i}(k,t) &= (7-i)h_B y P_{C_6B_{i-1}}(k,t) - i f_B P_{C_6B_i}(k,t) \\
&\quad -(6-i)h_B y P_{C_6B_i}(k,t) + (i+1) f_B P_{C_6B_{i+1}}(k,t), \quad \text{for } 1 \le i \le 5, \\
\frac{d}{dt}P_{C_6B_0}(k,t) &= -6h_B y P_{C_6B_0}(k,t) + f_B P_{C_6B_1}(k,t), \\
\frac{d}{dt}P_{C_6B_6}(k,t) &= h_B y P_{C_6B_5}(k,t) - 6 f_B P_{C_6B_6}(k,t),
\end{aligned} \qquad (3)$$

where y is the concentration of free unbound KaiB.

We describe the level of KaiC phosphorylation by a continuous variable $U_k(t)$; $U_k(t) \approx 1$ when all 12 sites in the CII ring are phosphorylated and $U_k(t) \approx -1$ when they are all unphosphorylated. Recent molecular dynamics simulations showed that binding KaiA to the CII ring changes the ring's structure, opening the pathway for ADP to exit the ring.[39] Therefore, the KaiA binding should increase the turnover of ATPase reactions in the CII ring, promoting Thr432 or Ser431 phosphorylation, while unbinding should increase the probability of bound ADP catalyzing Thr432 or Ser431 dephosphorylation. We describe these effects of KaiA binding/unbinding on P/dP reactions with the following equation for $U_k(t)$;

$$\frac{d}{dt}U_k = k_p P_{\mathrm{C_6A_2}}(k,t) - k_{dp}(1 - P_{\mathrm{C_6A_2}}(k,t)) - \frac{d}{dU_k}g(U_k), \qquad (4)$$

where k_p and k_{dp} are constants, and $g(U) = \frac{a}{4}(U^4 - U^2)$ is a soft-spin constraint, which confines $U_k(t)$ to a range of approximately -1 to 1. Here, we should note that Eq. 4 need not satisfy the detailed balance condition because the non-equilibrium ATP consumption in the CII domains is implicitly represented by k_p and k_{dp}.

Indirect interaction through KaiA sequestration. We solved Eqs. 2 and 3 numerically under the normalization condition,

$$1 = P_{\mathrm{C_6A_2}}(k,t) + \sum_{i=0}^{6} P_{\mathrm{C_6B}_i}(k,t), \qquad (5)$$

and the following constraints enforcing total KaiA and KaiB conservation in the solution:

$$A_T/2 = x + \frac{1}{V}\sum_{k=1}^{N} P_{\mathrm{C_6A_2}}(k,t) + \frac{g_{BA}x}{1 + g_{BA}x}\frac{1}{V}\sum_{k=1}^{N}\sum_{i=1}^{6} iP_{\mathrm{C_6B}_i}(k,t),$$

$$B_T = y + \frac{1}{V}\sum_{k=1}^{N}\sum_{i=1}^{6} iP_{\mathrm{C_6B}_i}(k,t). \qquad (6)$$

Here, A_T and B_T are the total concentrations of KaiA and KaiB on a monomer basis, V is the system volume, and N is the number of simulated KaiC hexamers in the system. See Supporting Information. The KaiC hexamer concentration is $C_{6T} = N/V$ and the total KaiC concentration is $C_T = 6N/V$, again on a monomer basis. Here, $g_{BA} = h_{BA}/f_{BA}$, where h_{BA} and f_{BA} are the binding and unbinding rate constants for KaiA to/from KaiB, respectively. In the binding/unbinding processes for KaiA to/from KaiB, we assume that the rate constants do not depend on the KaiC structure $W(k,t)$ because they do not involve any direct interactions between KaiA and KaiC; therefore, g_{BA} in Eq. 6 is a constant, independent of $W(k,t)$.

We should also note that Eqs. 2–6 do not include terms representing direct interactions between KaiC hexamers. Instead, we have a constraint that ensures conservation of the total KaiA concentration (Eq. 6). With this constraint, as long as A_T

is not too large, there is competition to bind the free unbound KaiA dimers between the CII rings and C_6B_i complexes. When some KaiC molecules have large affinity to bind KaiA to C_6B_i, or KaiA is sequestered in the KaiCBA complexes, then the free unbound KaiA in the solution is depleted, preventing KaiA binding to the CII rings of other KaiC molecules. This competition to consume the free KaiA leads to the indirect interactions among KaiC hexamers. In the Results and Discussion section, we will show that this KaiA sequestration mechanism is necessary to synchronize the oscillations of many KaiC molecules.

Regulation of allosteric structural changes by reactions. Because the allosteric structure changes of proteins take place in a timescale of milliseconds to seconds in many cases,[40] we also assume that the dynamics of $W(k,t)$ are much faster than the other slow reactions, such as P/dP, KaiB binding/unbinding, and ATPase reactions, which occur on a timescale of hours. Therefore, the structural state is in a quasi-equilibrium determined by the phosphorylation state and the binding states of KaiA, KaiB, and the nucleotides. Then, the structure state can be represented in a mean-field manner in the quasi-equilibrium description of $W(k,t)$ as

$$W(k,t) = \tanh\left[\beta\left(c_0 - c_1U_k + c_2p_k^{CA}(t) - c_3p_k^{CB}(t) - q_k(t)\right)\right], \qquad (7)$$

where $\beta = 1/k_BT$, U_k is the phosphorylation level, $p_k^{CA}(t) = P_{C_6A_2}(k,t)$ is the extent of the KaiA binding to the CII ring, $p_k^{CB}(t) = \sum_{i=1}^{6} P_{C_6B_i}(k,t)$ is the extent of the KaiB binding to the CI domains, and $q_k(t)$ represents the effect of ADP binding to the CI domains. In Eq.7, U_k, $p_k^{CA}(t)$, $p_k^{CB}(t)$, and $q_k(t)$ are treated as effective force fields in determining $W(k,t)$; See Supporting Information for further discussion.

Eq. 7 represents multifold feedback relations among reactions and structure: for example, the term $-c_1U_k$ ($c_1 > 0$) represents the tendencies of phosphorylated and unphosphorylated KaiC to form cs and gs structures, respectively. Because phosphorylation is enhanced in the gs structure through KaiA binding to the CII ring, as shown in Eqs.1 and 4, the term $-c_1U_k$ provides negative feedback effect. Meanwhile, the term $c_2p_k^{CA}(t)$ ($c_2 > 0$) represents positive feedback, because KaiA binding stabilizes the gs structure (Eq. 7), which in turn further increases KaiA binding to the CII ring (Eqs. 1 and 2). Similarly, the term $-c_3p_k^{CB}(t)$ ($c_3 > 0$) provides positive feedback because KaiB binding stabilizes the cs structure (Eq. 7), which in turn further increases KaiB binding (Eqs. 1 and 3). Figure 4 summarizes these multifold feedback relationships.

Due to these multifold feedback relations, KaiC hexamers can adopt multiple stationary states, including the large-p_k^{CA}/ large-W state and large-p_k^{CB}/ small-W state. The ATPase reactions represented by the term $-q_k(t)$ perturb the KaiC hexamers away from these stationary states, driving their oscillations. As we can see from Figure 4, allosteric structure transitions play a central role in creating the feedback relationships in individual KaiC hexamers.

Stochastic ATP hydrolysis in individual molecules. We represent the effect of nucleotides binding to the CI domain of the *i*th subunit of the *k*th KaiC hexamer at time *t* by the quantities $q(i;k,t)$ and $q_k(t) = \sum_{i=1}^{6} q(i;k,t)$. As shown in Eq. 7, the cs structure is stabilized in the present model when $q_k(t) > 0$.

It has been reported that ATP hydrolysis in the CI domain is necessary for KaiB to bind to KaiC.[36,38,41,42] Here, this is represented by the tendency of the ATP hydrolysis to stabilize the cs structure, promoting KaiB binding to KaiC. However it has been shown that ATP must bind to the CI domains to prevent KaiC hexamers dissociating into

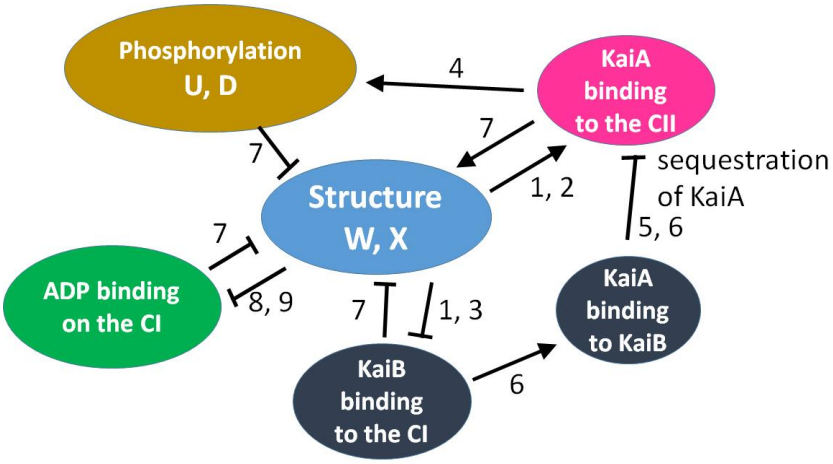

Figure 4. Relations among structure and reactions of KaiC hexamers, as defined by the multifold feedback model. Reactions are linked by arrows when one reaction stimulates the other, and the associated numbers relate to the equation numbers in the text. When the structure with the larger *W* value (*X* in the Results and Discussion section) is associated with the reaction, they are connected by conventional arrows, while the T-shaped arrows indicate cases where the structure with the smaller *W* (or *X*) value is associated with the reaction. These structure/reaction links constitute multifold feedback loops, and allosteric structural changes play a central role in creating these loops.

monomers;[6] therefore, it is reasonable to assume that ATP binding does not stabilize the cs structure but the cs structure is stabilized when ATP is hydrolyzed to ADP and inorganic phosphate (P_i). Therefore, we set $q(i;k,t) = 0$ when either ATP is bound or no nucleotides are bound, and $q(i;k,t) = q_0 > 0$ when either ADP and P_i are bound or ADP is bound on the CI domain of the *i*th subunit of the *k*th KaiC hexamer at time *t*.

We also assume that the frequency of ATP hydrolysis, i.e., the frequency with which $q(i;k,t)$ switches from 0 to q_0, depends on the structure $W(k,t)$. Because P_i, which is generated by ATP hydrolysis in the CII ring, is used for phosphorylation there, the frequency of such ATP hydrolysis should be higher in the P-phase than in the dP-phase. Here, we assume that ATP hydrolysis in the CI domains follows the opposite pattern to compensate for the large phosphorylation-level-dependent ATPase activity modulation in the CII rings and thereby reproduce the observed mild modulation in full-length KaiC;[31] the frequency of ATP hydrolysis in the CI domains is higher in the dP-phase, or cs-structure, so it depends on $W(k,t)$ as

$$f_k(t) = f_0\big(1 - \tanh(W(k,t)/C_W)\big), \qquad (8)$$

where C_W and f_0 are constants.

Release of the bound ADP from the CI should also be a stochastic event. For simplicity, we assume that ADP is released multiple times from the same molecule in an uncorrelated way, so that the ADP bound state lifetime for any given subunit of the *k*th KaiC hexamer follows a Poisson distribution with a lifetime Δ_k defined by $\Delta_k = \overline{\Delta}_k(t) + \xi_k(t)$, where ξ_k is a random number satisfying $\langle \xi_k(t) \rangle = 0$ and $\langle \xi_k(t)\xi_l(t') \rangle = \delta_{kl}\delta_{tt'}\overline{\Delta}_k(t)$. By introducing the constants C_W and δ_0, we define the average lifetime $\overline{\Delta}_k(t)$ as

$$\overline{\Delta}_k(t) = \delta_0\big(1 - \tanh(W(k,t)/C_W)\big). \qquad (9)$$

With this definition of $\overline{\Delta}_k$, the lifetime of the ADP bound state is longer in the cs structure. Therefore, from definitions of Eqs. 8 and 9, ADP binding has a more significant effect on cs-KaiC than gs-KaiC, as explained in Figure 4. In the Results and Discussion section, we show that this enhanced ADP binding in cs-KaiC is important for producing coherent oscillation in the present model.

In summary, we simulate ATP hydrolysis in the CI domains as stochastic events in individual subunits of KaiC hexamers. In our model, ATP hydrolysis takes place with the probability f_k (Eq. 8) in unit time. If it takes place at time $t = t_0$ in the *i*th subunit of

the kth KaiC hexamer, $q(i;k,t_0)$ changes from 0 to q_0. Then, the ADP (or ADP and P_i) remains bound during the interval $t_0 < t < t_0 + \Delta_k$. When ADP is finally released from the CI domain at time $t = t_0 + \Delta_k$, $q(i;k,t_0+\Delta_k)$ returns from q_0 to 0.

We should note that an alternative model is to assume $q(i;k,t_0) = 0$ when the ATP (or ADP and P_i) is bound in the CI domain, and $q(i;k,t_0)$ changes from 0 to q_0 when the P_i is released, remaining at q_0 while the ADP is bound. We do not currently have the evidence needed to decide between these two scenarios, but both scenarios (the one where $q(i;k,t_0) = q_0$ when either ADP+ P_i or ADP is bound and the other where $q(i;k,t_0) = q_0$ only when ADP is bound) yield the same mathematical expression in the present model; therefore, the model can be applied to either scenario and we will leave assessing the validity of these scenarios as a topic for future work.

Parameters. The model shows robust oscillations for a wide range of parameter values. In our simulations (refer the Results and Discussion section), we did not calibrate the parameter values to precisely reproduce the experimental data, but instead used values with one effective digit, to emphasize that precise calibration is not necessary to produce the important features of oscillations. We used the following parameter values, unless specified otherwise.

We simulated a system of $N = 1000$ KaiC hexamers. Therefore, in units of $V = 1$, we had $C_{6T} = 1000$ (i.e., $C_T = 6000$). Most of the following calculations assume KaiA and KaiB concentrations of $A_T = 2000$ and $B_T = 6000$, respectively on a monomer basis. This ratio, i.e., $A_T : B_T : C_T = 1 : 3 : 3$, has been often used in in vitro experiments.[9,31,38] In units of $V = 3 \times 10^{-15} l$, we have $C_T = 3.3\ \mu$M, which is close to the $3.5\ \mu$M concentration often used in experiments.

Most of the reaction rates in the model were assumed to be of the order of 1/hour. In units of $V = 1$, the binding rate constant for KaiB was chosen to make $h_{B0} B_T \approx 1\ \mathrm{h}^{-1}$, so that we assumed $h_{B0} = (1/3) \times 10^{-4}\ \mathrm{h}^{-1}$. The dissociation rate constant of KaiB was $f_{B0} = 3 \times 10^{-1}\ \mathrm{h}^{-1}$. The P/dP rate constants were $k_p = 3 \times 10^{-1}\ \mathrm{h}^{-1}$ and $k_{dp} = 2 \times 10^{-1}\ \mathrm{h}^{-1}$. The frequency of ATP hydrolysis was $f_0 = 1\ \mathrm{h}^{-1}$ and the lifetime of the ADP bound state was $\delta_0 = 2$ h except when we used $\delta_0 = 1$ h to calculate the data in Figure 8. The rate constant to define the soft-spin constraint was $a = 5 \times 10^{-1}\ \mathrm{h}^{-1}$. The binding/unbinding of KaiA was assumed to be much faster than other reactions; therefore, it was defined by the association constants $g_{A0} = h_{A0}/f_{A0}$ and $g_{BA} = h_{BA}/f_{BA}$. Here, we chose the values $g_{A0} = g_{BA} = 6 \times 10^{-3}$ (in $V = 1$ units), so as to set $g_{A0} A_T/2 \approx g_{BA} A_T/2 \approx 1$. In Eq. 7, the quasi-equilibrium equation that determines the structure, we set the structure/reaction coupling coefficients to be several $k_B T$ as $c_0 = 8 k_B T$, $c_1 =$

$6k_BT$, $c_2 = 2k_BT$, $c_3 = 6k_BT$, and $q_0 = 2k_BT$. The other constants relating the reaction rates to the structure were set to $A_W = B_W = C_W = 1$.

Simulation. At the start time t, initial values for the unbound free KaiA dimer concentration $x(t)$, the unbound free KaiB concentration $y(t)$, structural states $W(k,t)$, phosphorylation levels $U_k(t)$, and probabilities of Kai protein association $P_{C_6B_i}(k,t)$ were given for $k = 1 \sim N$ and $i = 1 \sim 6$. The nucleotide binding states, $q(i;k,t)$, were set to 0. The initial rate constants were calculated using Eq. 1 and the $P_{C_6A_2}(k,t)$ were calculated using Eq. 2.

Then, $U_k(t+\Delta t)$ and $P_{C_6B_i}(k,t+\Delta t)$ were calculated by numerically integrating Eqs. 3 and 4 with a time step $\Delta t = 10^{-3}$ h, and the $P_{C_6A_2}(k,t+\Delta t)$ were recalculated with Eq. 2, with the $P_{C_6B_i}(k,t+\Delta t)$ and $P_{C_6A_2}(k,t+\Delta t)$ being rescaled to satisfy the normalization condition Eq. 5. Then, by solving Eq. 6, values of $x(t+\Delta t)$ and $y(t+\Delta t)$ were obtained. The frequencies of ATP hydrolysis $f_k(t+\Delta t)$ in Eq. 8 were calculated, and the randomly distributed lifetimes of the ADP bound state Δ_k, were calculated with the mean value determined by Eq. 9. Then, the $q(i;k,t+\Delta t)$ were changed from 0 to q_0 with probability $f_k\Delta t$ and, where the values changed, the new values were retained for the following $\Delta_k/\Delta t$ steps. Finally, the $U_k(t+\Delta t)$, $P_{C_6A_2}(k,t+\Delta t)$, $P_{C_6B_i}(k,t+\Delta t)$ and $q(i;k,t+\Delta t)$ were used to calculate the structure $W(k,t+\Delta t)$ with Eq. 7. This process was repeated to calculate the trajectory of the dynamics. The oscillation frequency was calculated by Fourier transforming a trajectory of the length 0.1×2^{15} h.

Results and Discussion

In this section, we explain the results simulated with the multifold feedback model of the KaiABC system having $N = 1000$ KaiC hexamers. In order to compare the calculated results with those obtained with our previous model,[29,30] we convert the quantities defined in the range -1 to 1 in the last section to lie between 0 and 1 as

$$D_k(t) = \frac{U(k,t)+1}{2}, \quad \bar{D}(t) = \frac{1}{N}\sum_{k=1}^{N} D_k(t), \qquad (10)$$

and

$$X_k(t) = \frac{W(k,t)+1}{2}, \quad \bar{X}(t) = \frac{1}{N}\sum_{k=1}^{N} X_k(t), \qquad (11)$$

where $D_k(t)$ is the phosphorylation level of the kth KaiC hexamer, $\bar{D}(t)$ is its average

over the ensemble, $X_k(t)$ is the structural order parameter of the kth KaiC hexamer, and $\bar{X}(t)$ is its average over the ensemble. We also define the ensemble average of probabilities that KaiC hexamers form complexes of KaiCA and KaiCB as

$$\bar{p}^{CA}(t) = \frac{1}{N}\sum_{k=1}^{N} p_k^{CA}(t), \quad \bar{p}^{CB}(t) = \frac{1}{N}\sum_{k=1}^{N} p_k^{CB}(t). \qquad (12)$$

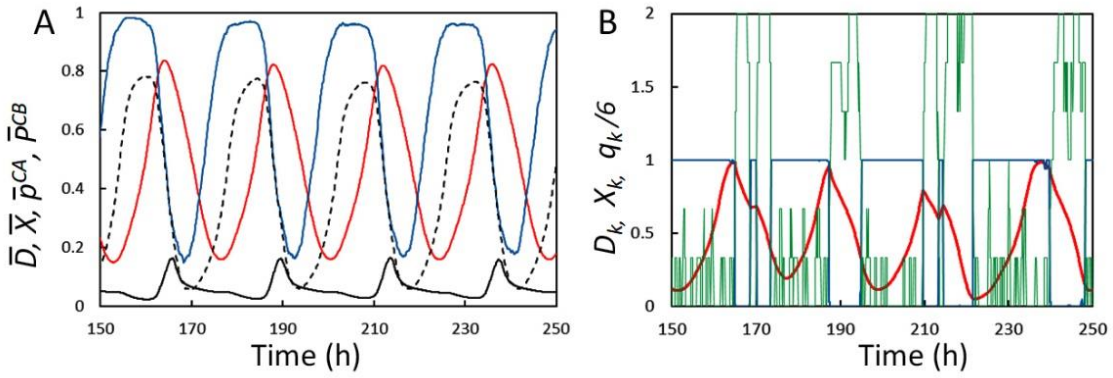

Figure 5. Simulated ensemble and single-molecule oscillations of KaiC. (A) Oscillations of the ensemble of KaiC hexamers. The level of phosphorylation $\bar{D}(t)$ (red), structural state $\bar{X}(t)$ (blue), probability to form KaiCA complex $\bar{p}^{CA}(t)$ (black dashed), and probability to form KaiCB complex $\bar{p}^{CB}(t)$ (black real) are plotted as functions of time t. (B) Oscillations of an example single KaiC hexamer in the ensemble. The level of phosphorylation $D_k(t)$ (red) and structural state $X_k(t)$ (blue) are plotted. The effect of ADP binding $q_k(t)/6$ (green) is plotted in units of $k_{\mathrm{B}}T$ whose maximum value is $q_0 = 2k_{\mathrm{B}}T$.

Ensemble and single-molecular oscillations. Shown in Figure 5A are dynamics of ensemble of many molecules. The ensemble exhibits stable oscillations in the phosphorylation level, structural state of KaiC, and probabilities to form KaiCA and KaiCB complexes with approximately 24-hour period. The structure is gs-like in the P-phase and cs-like in the dP-phase. The probability to form the KaiCA complex is large in the P-phase, while the probability to form the KaiCB complex is large in the dP-phase. Thus, we see the coherent coordination among the structural, Kai protein binding affinity, and phosphorylation level changes at the ensemble level.

These ensemble-level oscillations are made of the oscillations of many individual molecules, so distinct oscillations of individual molecules are required to realize coherent ensemble oscillations. Figure 5B shows the oscillation of a single example molecule. Each molecule undergoes stepwise changes between the gs and cs structures. In the gs structure with $X_k(t) \approx 1$, ATP hydrolysis provides a sequence of ADP binding spikes with $q_k(t) \neq 0$. However, each spike's lifetime is too short for this frequent binding to have any significant effect on the structure $X_k(t)$. By contrast, in the cs structure with $X_k(t) \approx 0$, the lifetime of the ADP bound state is much elongated as defined in Eq. 9, so that KaiC is saturated with bound ADP, stabilizing the cs structure through the effect described in Eq. 7. This positive feedback between ADP binding and structure change gives rise to switch-like transitions of structure. In isolated molecules, these transitions would take place randomly, but synchronization among molecules in the system regulates this intramolecular switching process to produce oscillations with a well-defined period.

Mechanism of synchronization. In the present model, synchronization is realized through sequestration of KaiA as discussed in the previous section. This effect can be clearly seen if we increase the KaiA concentration: when KaiA molecules are too abundant, KaiA sequestration becomes ineffective.

In Figure 6A, oscillations of five individual KaiC hexamers arbitrarily chosen from the system (i.e., $D_k(t)$ with five different ks) are shown together with the ensemble oscillation $\bar{D}(t)$. Here, the left panel of Figure 6A shows the oscillations for the standard ratio of concentrations, $A_T/C_{6T} = 2$ and $B_T/C_{6T} = 6$, where $C_{6T} = (1/6)C_T$ is the concentration of KaiC hexamer in the system. In this case, individual molecules oscillate in a highly synchronized manner, showing only slight fluctuations around the ensemble

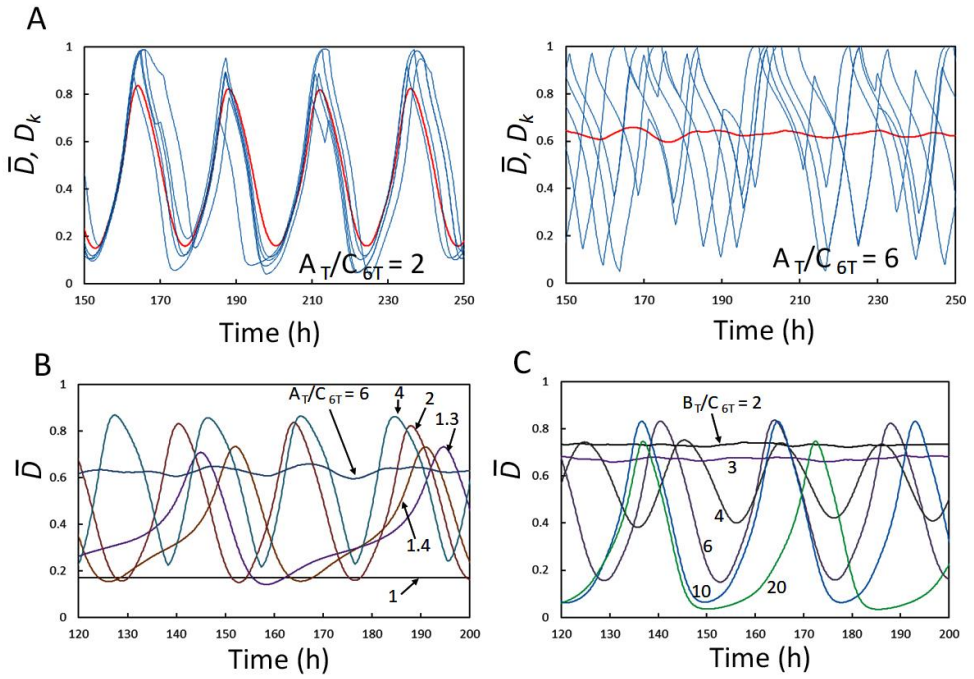

Figure 6. Simulated ensemble and single-molecule dynamics of phosphorylation level for different concentrations of KaiA and KaiB. (A) Phosphorylation level for the standard KaiA concentration, $A_T/C_{6T} = 2$ and $B_T/C_{6T} = 6$ (left), and an increased KaiA concentration, $A_T/C_{6T} = 6$ and $B_T/C_{6T} = 6$ (right). These plots show the ensemble-averaged phosphorylation level $\bar{D}(t)$ (red) and the phosphorylation levels of five example molecules $D_k(t)$ (blue). (B) $\bar{D}(t)$ calculated for various A_T/C_{6T} at a fixed KaiB concentration $B_T/C_{6T} = 6$. (C) $\bar{D}(t)$ calculated for various B_T/C_{6T} at a fixed KaiA concentration $A_T/C_{6T} = 2$.

average. By contrast, as shown in the right panel of Figure 6A, oscillations of $\bar{D}(t)$ vanish when we increase the KaiA concentration to $A_T/C_{6T} = 6$. With such a large concentration of KaiA, the individual KaiC hexamers oscillate with large amplitudes as shown in examples of $D_k(t)$, but their oscillatory phases are uncorrelated to each other, reducing the $\bar{D}(t)$ oscillations. With this large concentration of KaiA, sequestration of KaiA is ineffective and synchronization is lost.

Dependence of the ensemble oscillation on the concentration of KaiA is shown in Figure 6B. By keeping $B_T/C_{6T} = 6$, various different A_T/C_{6T} values were tested. As the KaiA concentration drops below the standard concentration $A_T/C_{6T} = 2$, the phosphorylation rate reduces and the oscillation period increases. When the KaiA concentration is $A_T/C_{6T} < 1$, the phosphorylation rate becomes too small to maintain

the oscillations. By contrast, as the KaiA concentration rises above the standard value, the phosphorylation rate increases and the oscillation period reduces. When $A_T/C_{6T} > 6$, the ensemble oscillation disappears, due to the individual oscillations losing synchronization, as shown in Figure 6A. Qualitatively similar behavior was observed experimentally:[43] the phosphorylation stayed at a low level and the oscillations stopped for $A_T/C_{6T} < 0.5$, and the oscillations also disappeared for $A_T/C_{6T} > 8$. This observed and simulated disappearance of oscillations at high concentration of KaiA is consistent with the idea that the sequestration of KaiA is necessary for synchronization.

Here, we briefly summarize the effects of KaiA sequestration on synchronization. When KaiB binds to some population of KaiC hexamers in the dP-phase and then KaiA binds to these KaiCB complexes, the concentration of free unbound KaiA decreases. This depletion of free KaiA decreases the rate at which KaiA binds to the other KaiC hexamers, which delays the P-reactions of those hexamers. In this way, a lowly phosphorylated KaiC population accumulates when KaiA is sequestrated by a certain amount of KaiCBA complexes, leading to synchronized oscillations of many KaiC molecules. However, when the system contains too many KaiA molecules as shown in Figure 6, this effect is less significant and the synchronization eventually disappears. The present simulation showed that due to the large capacity of each KaiCBA complex to accommodate a large number of KaiA dimers (up to six), the effect of KaiA sequestration in KaiCBA complexes is sufficient and there is no need to assume other mechanisms, such as sequestration in other specific KaiC states or monomer exchange.

Dependence of the ensemble oscillations on the KaiB concentration is shown in Figure 6C. When the concentration is too low ($B_T/C_{6T} < 3$), the rate of dephosphorylation is so small that the phosphorylation stays high without showing oscillation. However, oscillations appear as B_T/C_{6T} increases and are maintained even at high concentration of $B_T/C_{6T} = 20$. This simulated behavior agrees qualitatively with the observations,[43] which showed no oscillations and high phosphorylation level for $B_T/C_{6T} < 1.5$, with oscillations appearing when the KaiB concentration was increased to $B_T/C_{6T} = 3$ and continuing with only slight changes as the concentration was increased to $B_T/C_{6T} = 30$. This simulated and observed maintenance of oscillations at high KaiB concentrations is because depleting the amount of free unbound KaiB is not necessary for synchronization.

Synchronization is also promoted by ATP hydrolysis. Figure 7 shows how the oscillations depend on the frequency parameter f_0 of ATP hydrolysis in the CI domains. As the frequency is decreased without changing other parameters, amplitude of the ensemble oscillations $\overline{D}(t)$ decreases. At around $f_0 \approx 0.5$, the amplitudes of

oscillations of individual molecules are still large but they are not well synchronized, which makes the ensemble oscillation amplitude small. The ADP binding in the CI perturbs the structure, which triggers the transition of structure from gs to cs in the present model. As ATP hydrolysis becomes infrequent, structural transitions become infrequent and individual molecules fail to follow the ensemble-level oscillations, which leads to desynchronization. By further decreasing the frequency of ATP hydrolysis, structural transitions become further infrequent, which suppresses individual oscillations and the phosphorylation level becomes to stay at a high value. Therefore, our model suggests

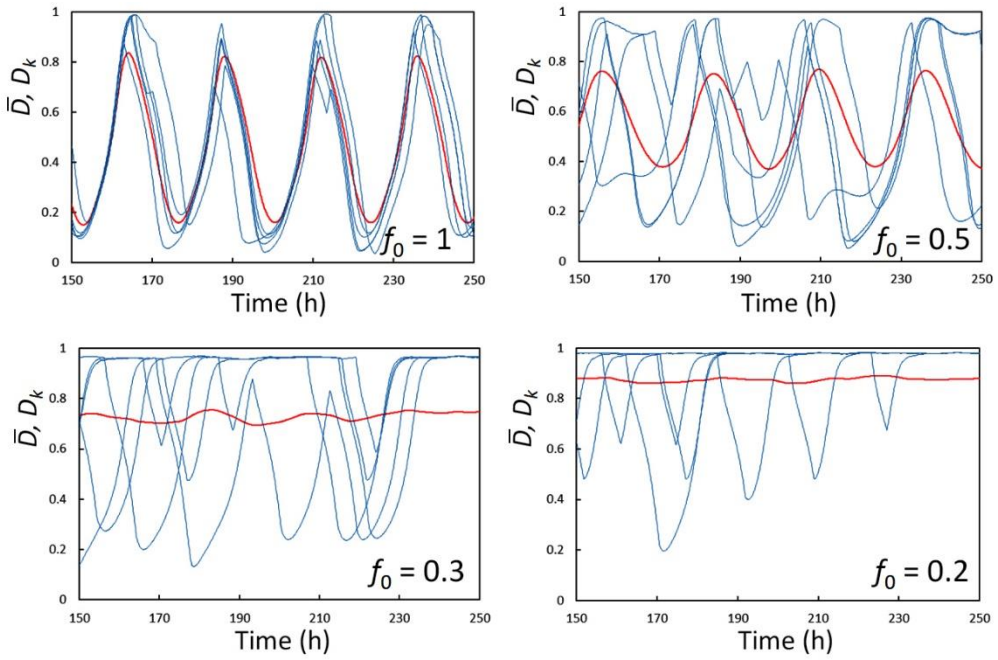

Figure 7. Simulated ensemble and single-molecule dynamics of the phosphorylation level for different frequency parameter f_0 of ATP hydrolysis. The ensemble-averaged phosphorylation level $\bar{D}(t)$ (red) and phosphorylation level of five example molecules in the ensemble $D_k(t)$ (blue) are superposed. Values of f_0 in the figure are in units of h^{-1}. $f_0 = 1\ \mathrm{h}^{-1}$ in the standard parameterization in the present paper.

that ATP hydrolysis in the CI domains assists synchronization, with synchronization being lost when the ATP hydrolysis frequency is too low.

We should note that ATP hydrolysis in the CI domains perturbs the structure of KaiC hexamers in the present model. At large f_0, gs-KaiC experiences frequent structural

perturbations, as shown by the trains of q_k spikes in Figure 5B. With these frequent perturbations, the KaiC molecules flexibly respond to structural transition cues, such as KaiB binding or KaiA unbinding. By contrast, when these structural perturbations are less frequent, the KaiC hexamers do not respond to such ques, and hence individual molecules are less able to adjust their oscillations to match those of the ensemble. Our model therefore suggests that ATP hydrolysis in the CI domains assists synchronization, with synchronization being lost when the ATP hydrolysis frequency is too low.

Correlation between ATPase activity and oscillation frequency. As shown in Figure 5B and Figure 7, ATP hydrolysis in the CI domains plays an important role in both the oscillations of individual molecules and the ensemble-level oscillations. We can analyze this further by calculating the correlation between the P/dP oscillation frequency and the ATPase activity.

In Figure 8, the ATPase activity is defined as the number of ADP molecules released from the CI domain per day per subunit calculated under the steady state condition $A_T = B_T = 0$. Here, we calculated the ATPase activity and the P/dP oscillation frequency for

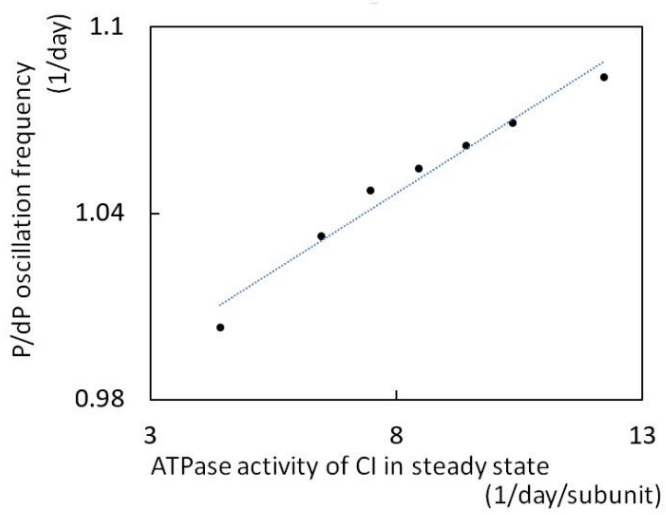

Figure 8. Correlation between ATPase activity and the frequency of phosphorylation/dephposphorylation oscillations of the ensemble of molecules. The ATPase activity was calculated as the average number of ADP molecules released from the CI domain of one subunit per day under a stationary condition without KaiA or KaiB. Plotted by varying f_0 from $0.8\,\mathrm{h}^{-1}$ to $2.4\,\mathrm{h}^{-1}$ with $\delta_0 = 1$ h.

ATP hydrolysis frequency f_0 from $f_0 = 0.8\,\mathrm{h}^{-1}$ to $2.4\,\mathrm{h}^{-1}$. Although the slope of the fitted line in this plot is 0.01, which is smaller than the experimentally observed slope of about 0.03,[32] the simulated results showed that the steady-state ATPase activity is clearly correlated with the oscillation frequency in our model. The model thus qualitatively reproduces the key observation that ATP hydrolysis in the CI, which should take place stochastically in individual molecules, strongly affects the ensemble-level oscillations.

The slope of correlation in Figure 8 depends on the parameterization: with $\delta_0 = 2$ h, we have a clear correlation with a slop value of around 0.02. To reproduce further quantitative features of the observed correlation, including the slope, we would need to consider the cooperativity and nonlinearity of intramolecular dynamics in more detail, including the cooperativity of the repeated ATP hydrolysis reactions taking place in subunits of the hexamer. Further detailed analyses of various KaiC mutants would assist such an investigation.

Dependence of oscillations on reaction rates. ATP hydrolysis in the CI domains, which takes place stochastically in individual molecules, drives structural transitions in those molecules through positive feedback between ADP binding and structural transitions. These transitions drive oscillations of individual molecules and are also required to synchronize many molecules by preventing stacking of each molecule to a particular structural state. The importance of these effects of ATP hydrolysis is evident in the simulated correlation between ATPase activity in the CI domains and the frequency of the ensemble oscillations. These results obtained with the present model are qualitatively similar to those found with our previous model, in which the rates of KaiA binding/unbinding reactions were very slow.[29,30] In other words, the main results of the multifold feedback model remain unchanged even when the rates of KaiA binding/unbinding change by orders of magnitude, as long as the association constants, g_A and g_{BA}, do not change significantly.

It is interesting to examine whether the model is as robust to changes in other reaction rates. In Figure 9A, the ensemble oscillations $\overline{D}(t)$ are shown for various values of rate constants of KaiB binding/unbinding reactions; the unbinding rate constant f_{B0} and the binding rate constant h_{B0} were changed while maintaining the ratio $g_B = h_{B0}/f_{B0} = (1/9) \times 10^{-3}$ in units of $V = 1$. The ensemble oscillations diminish when

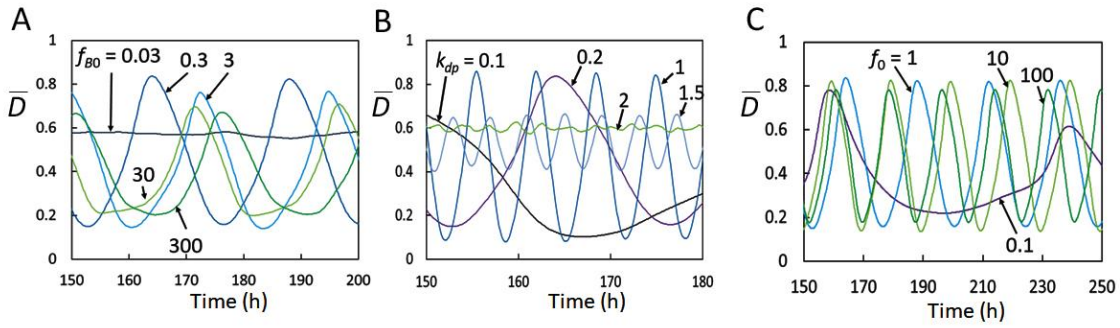

Figure 9. Simulated ensemble dynamics of the phosphorylation level for various different values of reaction rate constants. (A) Ensemble-averaged phosphorylation level $\overline{D}(t)$ for different values of rate constants of binding/unbinding of KaiB; f_{B0} and h_{B0} were varied while keeping $g_B = h_{B0}/f_{B0}$ constant. (B) $\overline{D}(t)$ for different values of rate constants of phosphorylation/dephosphorylation; k_{dp} and k_p were varied while keeping k_{dp}/k_p constant. (C) $\overline{D}(t)$ for different values of frequency parameter of ATP hydrolysis f_0 and the lifetime parameter of ADP bound state δ_0; f_0 and δ_0 were varied while keeping $f_0\delta_0$ constant. Values of rate constants in the figure are in units of h^{-1}

f_{B0} and h_{B0} are too small, but as log as $f_{B0} > 0.1\ \mathrm{h}^{-1}$, the oscillation features do not change significantly over a wide range of f_{B0} and h_{B0} values. This shows that the ensemble oscillations are robust against changes in the KaiB binding/unbinding rate constants; to obtain coherent oscillations, there appears to be no need to tune the KaiB binding/unbinding rates precisely, which could be evaluated experimentally by testing mutants of KaiB.

By contrast, the oscillations are highly sensitive to the P/dP rates, as shown in Figure 9B, where the phosphorylation and dephosphorylation rates k_p and k_{dp} were changed while maintaining the ratio $k_{dp}/k_p = 2/3$. Here, the oscillation period shortens as k_p and k_{dp} increase and the ensemble oscillations disappear when $k_{dp} > 2\ \mathrm{h}^{-1}$. Conversely, the period lengthens as k_p and k_{dp} decrease and the oscillations cease when $k_{dp} < 0.05\ \mathrm{h}^{-1}$. Because the P_i provided by ATP hydrolysis in the CII domains is used for phosphorylation, and their bound ADP is used for dephosphorylation,[44,45] k_p and k_{dp} should be determined by the rates of ATP hydrolysis reactions in the CII domains. The present result suggests that k_p and k_{dp} need to be tuned within a certain range to produce coherent oscillations, and that this tuning could be realized through the evolutionary design of the ATPase activity in the CII domains. This picture is consistent

with the results of molecular dynamics simulations showing that the rate of ATPase reactions is determined by structure tuning.[39]

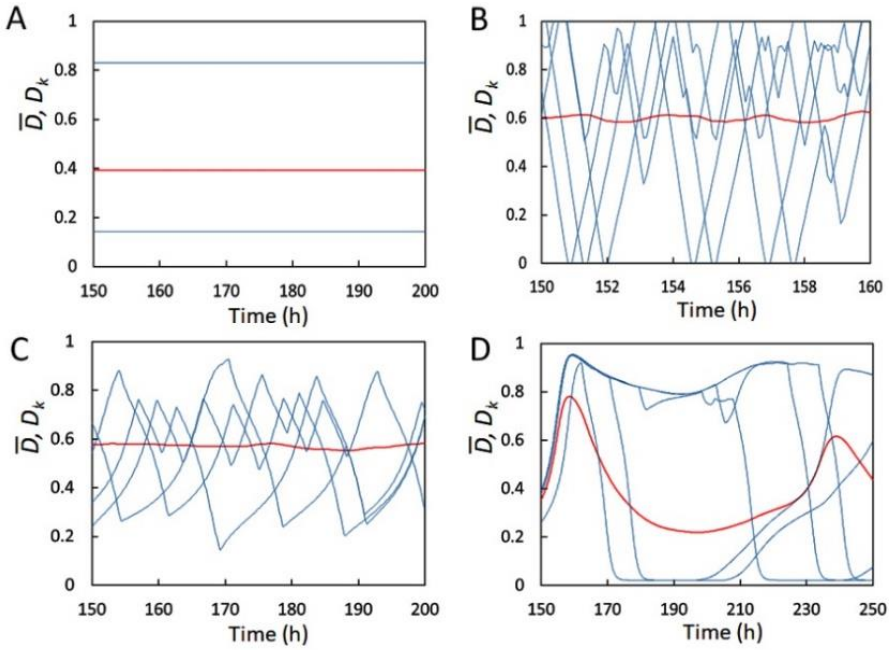

Figure 10. Simulated ensemble and single-molecule dynamics of the phosphorylation level in several cases where the ensemble oscillations disappear. The ensemble-averaged phosphprylation level $\overline{D}(t)$ (red) and the phosphorylation level of five example molecules in the ensemble $D_k(t)$ (blue) are superposed. Calculated for (A) small phosphorylation/dephosphorylation rate constants; $k_p = 0.03\ \mathrm{h}^{-1}$ and $k_{dp} = 0.02\ \mathrm{h}^{-1}$, (B) large phosphorylation/dephosphorylation rate constants; $k_p = 3\ \mathrm{h}^{-1}$ and $k_{dp} = 2\ \mathrm{h}^{-1}$, (C) small binding/unbinding rate constants of KaiB; $f_{B0} = 0.03\ \mathrm{h}^{-1}$ and $h_{B0}=(1/3)\times 10^{-5}\ \mathrm{h}^{-1}$, and (D) small frequency parameter of ATP hydrolysis and large lifetime parameter of ADP bound state; $f_0 = 0.1\ \mathrm{h}^{-1}$ and $\delta_0 = 20$ h.

As the probability of the ADP remaining bound on the CI domains is determined by $f_0\delta_0$, and the effect of the ADP bound state to the structural changes depends largely on this probability, the oscillation feature should not be sensitive to changes of f_0 and δ_0 as long as $f_0\delta_0$ remains constant. Figure 9C shows the ensemble oscillations for various values of the frequency parameter of ATP hydrolysis f_0 and the typical lifetime of the ADP bound state δ_0, with f_0 and δ_0 being changed simultaneously while

maintaining $f_0\delta_0 = 2$. With $f_0 = 0.1\ \mathrm{h}^{-1}$ and $\delta_0 = 20\ \mathrm{h}$, the ensemble-level dynamics become irregular, showing a slow temporal change. However, the oscillations are clear for $f_0 = 1\ \mathrm{h}^{-1}$, and the oscillation features do not depend significantly on f_0 or δ_0 when $f_0 > 1\ \mathrm{h}^{-1}$ if $f_0\delta_0$ is kept constant.

It is intriguing to analyze the reasons why the ensemble oscillations disappear in the above cases. One way to analyze this is to compare the ensemble dynamics $\overline{D}(t)$ with the individual-molecule dynamics $D_k(t)$. In Figure 10, $\overline{D}(t)$ and $D_k(t)$ of five arbitrarily chosen molecules are plotted for several pathological cases in which the ensemble oscillations disappear. Figure 10A shows a case of slow P/dP reactions with $k_p = 0.03\ \mathrm{h}^{-1}$ and $k_{dp} = 0.02\ \mathrm{h}^{-1}$. With such small rate constants, owing to the timescale difference among reactions, structural changes and P/dP reactions are not coordinated and each molecule stays in one of two stable states, the large-X_k/small-D_k state or the small-X_k/large-D_k state, with the ensemble value $\overline{D}$ being their average. Conversely, in the case shown in Figure 10B, the P/dP reactions are fast with $k_p = 3\ \mathrm{h}^{-1}$ and $k_{dp} = 2\ \mathrm{h}^{-1}$. With such fast P/dP reactions, binding/unbinding of KaiB cannot keep up. Because binding of KaiB is necessary for KaiA sequestration and hence for synchronization, synchronization is lost in this case.

Figure 10C shows a case where binding/unbinding of KaiB is slow with $f_{B0} = 0.03\ \mathrm{h}^{-1}$ and $h_{B0} = (1/3) \times 10^{-5}\ \mathrm{h}^{-1}$. In the case of such slow rates of binding/unbinding, the KaiB binding/unbinding reactions cannot keep up wth the P/dP reactions and again leading to desynchronization. The oscillation pattern of Figure 10C is similar to that in Figure 10B although their timescales are different. This similarity between the patterns of Figures 10C and 10B should arise from the same reason for desynchronization in both cases, the mismatch of timescales of KaiB binding/unbinding and P/dP reactions. This similarity suggests we need $f_{B0}/k_p \gtrsim 0.2$ to achieve stable ensemble-level oscillations, and that individual molecules become desynchronized when $f_{B0}/k_p < 0.1$.

Finally, Figure 10D shows the case where $f_0 = 0.1\ \mathrm{h}^{-1}$ and $\delta_0 = 20\ \mathrm{h}$. Here, ATP hydrolysis only infrequently induces structural transitions and their stochastic nature appears clearly in the dynamics, meaning that the molecular changes are irregular. This shows that we need multiple ADP bindings over the course of a single dP-phase to avoid stochastic, irregular structural transitions appearing in the ensemble dynamics.

Conclusions

In this study, we have developed a coarse-grained model of the structure and reactions of

Kai molecules and described the ensemble oscillations of KaiC molecules, which are realized by synchronizing the oscillations of many individual KaiC molecules. In our simulations, we found that the KaiC hexamer oscillations are driven by switch-like allosteric structural transitions in individual hexamers, induced by positive feedback between structural changes and ATP hydrolysis in the CI domains. The simulation results based on the assumption of sequestration of KaiA into KaiCBA complex was consistent with the observed data of dependence of oscillations on concentrations of KaiA and KaiB.

We have shown that ATP hydrolysis in the CI domains at frequencies above a certain threshold is necessary for individual molecules to flexibly adjust to the averaged oscillations of ensemble, so that they desynchronize if ATP hydrolysis is too infrequent. Thus, ATP consumption in the CI domains appears to be necessary to achieve coherent ensemble-level oscillations. These results suggest an important role of ATP hydrolysis in the ensemble oscillations, which is consistent with the simulated and observed correlation between oscillation frequency and ATPase activity. The ensemble oscillations are robust against changes in reaction rates: they persist even when the KaiA or KaiB binding/unbinding rates change substantially as long as the association constant values are maintained. However, the oscillations are sensitive to changes in P/dP reaction rates, although further analyses at an atomic resolution will be needed to clarify the mechanism by which these rates are tuned.[32,39]

In summary, our newly developed coarse-grained model, the multifold feedback model, suggested mechanisms of oscillations and synchronization, which should assist in further analyzing the relationship between single- and many-molecule dynamics in this oscillatory system, as well as presenting a new perspective on the phenomena governed by the interplay between microscopic elementary processes and macro- or mesoscopic emergent dynamics.

Acknowledgements

This work was supported by the Riken Pioneering Project, JST CREST Grant Number JPMJCR15G2, and JSPS KAKENHI Grant Number JP16H02217.

References

(1) Nakajima, M.; Imai, K.; Ito, H.; Nishiwaki, T.; Murayama, Y.; Iwasaki, H.; Oyama, T.; Kondo, T. Reconstitution of circadian oscillation of cyanobacterial KaiC phosphorylation in vitro. *Science* **2005,** *308*, 414-415.

(2) Akiyama, S. Structural and dynamic aspects of protein clocks: how can they be so

slow and stable? *Cell Mol Life Sci* **2012,** *69*, 2147-2160.

(3) Egli, M. Intricate protein-protein interactions in the cyanobacterial circadian clock. *J Biol Chem* **2014,** *289*, 21267-21275.

(4) Iwasaki, H.; Taniguchi, Y.; Ishiura, M.; Kondo, T. Physical interactions among circadian clock proteins KaiA, KaiB and KaiC in cyanobacteria. *EMBO J* **1999,** *18*, 1137-1145.

(5) Mori, T.; Saveliev, S. V.; Xu, Y.; Stafford, W. F.; Cox, M. M.; Inman, R. B.; Johnson, C. H. Circadian clock protein KaiC forms ATP-dependent hexameric rings and binds DNA. *Proc Natl Acad Sci USA* **2002,** *99*, 17203-17208.

(6) Hayashi, F.; Suzuki, H.; Iwase, R.; Uzumaki, T.; Miyake, A.; Shen, J. R.; Imada, K.; Furukawa, Y.; Yonekura, K.; Namba, K.; et al. ATP-induced hexameric ring structure of the cyanobacterial circadian clock protein KaiC. *Genes Cells* **2003,** *8*, 287-296.

(7) Pattanayek, R.; Wang, J.; Mori, T.; Xu, Y.; Johnson, C. H.; Egli, M. Visualizing a circadian clock protein: crystal structure of KaiC and functional insights. *Mol Cell* **2004,** *15*, 375-388.

(8) Rust, M. J.; Markson, J. S.; Lane, W. S.; Fisher, D. S.; O'Shea, E. K. Ordered phosphorylation governs oscillation of a three-protein circadian clock. *Science* **2007,** *318*, 809-812.

(9) Nishiwaki, T.; Satomi, Y.; Kitayama, Y.; Terauchi, K.; Kiyohara, R.; Takao, T.; Kondo, T. A sequential program of dual phosphorylation of KaiC as a basis for circadian rhythm in cyanobacteria. *EMBO J* **2007,** *26*, 4029-4037.

(10) Ye, S.; Vakonakis, I.; Ioerger, T. R.; LiWang, A. C.; Sacchettini, J. C. Crystal structure of circadian clock protein KaiA from *Synechococcus elongatus*. *J Biol Chem* **2004,** *279*, 20511-20518.

(11) Pattanayek, R.; Williams, D. R.; Pattanayek, S.; Xu, Y.; Mori, T.; Johnson, C. H.; Stewart, P. L.; Egli, M. Analysis of KaiA-KaiC protein interactions in the cyano-bacterial circadian clock using hybrid structural methods. *EMBO J* **2006,** *25*, 2017-2028.

(12) Iwasaki, H.; Nishiwaki, T.; Kitayama, Y.; Nakajima, M.; Kondo, T. KaiA-stimulated KaiC phosphorylation in circadian timing loops in cyanobacteria. *Proc Natl Acad Sci USA* **2002,** *99*, 15788-15793.

(13) Snijder, J.; Schuller, J. M.; Wiegard, A.; Lössl, P.; Schmelling, N.; Axmann, I. M.; Plitzko, J. M.; Förster, F.; Heck, A. J. R. Structures of the cyanobacterial circadian oscillator frozen in a fully assembled state. *Science* **2017,** *355*, 1181-1184.

(14) Mori, T.; Sugiyama, S.; Byrne, M.; Johnson, C. H.; Uchihashi, T.; Ando, T. Revealing circadian mechanisms of integration and resilience by visualizing clock proteins

working in real time. *Nat Commun* **2018,** *9*, 3245.
(15) Kitayama, Y.; Iwasaki, H.; Nishiwaki, T.; Kondo, T. KaiB functions as an attenuator of KaiC phosphorylation in the cyanobacterial circadian clock system. *EMBO J* **2003,** *22*, 2127-2134.
(16) Xu, Y.; Mori, T.; Johnson, C. H. Cyanobacterial circadian clockwork: roles of KaiA, KaiB and the kaiBC promoter in regulating KaiC. *EMBO J* **2003,** *22*, 2117-2126.
(17) Emberly, E.; Wingreen, N. S. Hourglass model for a protein-based circadian oscillator. *Phys Rev Lett* **2006**, *96*, 038303.
(18) Takigawa-Imamura, H.; Mochizuki, A. Predicting regulation of the phosphorylation cycle of KaiC clock protein using mathematical analysis. *J Biol Rhythms* **2006,** *21*, 405-416.
(19) van Zon, J. S.; Lubensky, D. K.; Altena, P. R.; ten Wolde, P. R. An allosteric model of circadian KaiC phosphorylation. *Proc Natl Acad Sci USA* **2007,** *104*, 7420-7425.
(20) Hatakeyama, T. S.; Kaneko, K. Generic temperature compensation of biological clocks by autonomous regulation of catalyst concentration. *Proc Natl Acad Sci USA* **2012,** *109*, 8109-8114.
(21) Phong, C.; Markson, J. S.; Wilhoite, C. M.; Rust, M. J. Robust and tunable circadian rhythms from differentially sensitive catalytic domains. *Proc Natl Acad Sci USA* **2013,** *110*, 1124-1129.
(22) Wang, J.; Xu, L; Wang, E. Robustness and coherence of a three-protein circadian oscillator: Landscape and flux perspectives. *Biophys J* **2009**, *97*, 3038–3046.
(23) Mori, T.; Williams, D. R.; Byrne, M. O.; Qin, X.; Egli, M.; McHaourab, H. S.; Stewart, P. L.; Johnson, C. H. Elucidating the ticking of an in vitro circadian clockwork. *PLoS Biol* **2007,** *5*, e93.
(24) Yoda, M.; Eguchi, K.; Terada, T. P.; Sasai, M. Monomer-shuffling and allosteric transition in KaiC circadian oscillation. *PLoS One* **2007,** *2*, e408.
(25) Eguchi, K.; Yoda, M.; Terada, T. P.; Sasai, M. Mechanism of robust circadian oscillation of KaiC phosphorylation in vitro. *Biophys J* **2008,** *95*, 1773-1784.
(26) Nagai, T.; Terada, T. P.; Sasai, M. Synchronization of circadian oscillation of phosphorylation level of KaiC in vitro. *Biophys J* **2010,** *98*, 2469-2477.
(27) Paijmans, J.; Lubensky, D. K.; Ten Wolde, P. R. A thermodynamically consistent model of the post-translational Kai circadian clock. *PLoS Comput Biol* **2017,** *13*, e1005415.
(28) Kageyama, H.; Nishiwaki,T.; Nakajima,M.; Iwasaki, H.; Oyama, T.; Kondo, T. Cyanobacterial circadian pacemaker: Kai protein complex dynamics in the KaiC phosphorylation cycle in vitro. *Molecular Cell* **2006**, 23, 161–171.

(29) Das, S.; Terada, T. P.; Sasai, M. Role of ATP hydrolysis in cyanobacterial circadian oscillator. *Sci Rep* **2017,** *7*, 17469.
(30) Das, S.; Terada, T. P.; Sasai, M. Single-molecular and ensemble-level oscillations of cyanobacterial circadian clock. *Biophys Physicobiol* **2018,** *15*, 136-150.
(31) Terauchi, K.; Kitayama, Y.; Nishiwaki, T.; Miwa, K.; Murayama, Y.; Oyama, T.; Kondo, T. ATPase activity of KaiC determines the basic timing for circadian clock of cyanobacteria. *Proc Natl Acad Sci USA* **2007,** *104*, 16377-16381.
(32) Abe, J.; Hiyama, T. B.; Mukaiyama, A.; Son, S.; Mori, T.; Saito, S.; Osako, M.; Wolanin, J.; Yamashita, E.; Kondo, T.; Akiyama, S. Atomic-scale origins of slowness in the cyanobacterial circadian clock. *Science* **2015,** *349*, 312-316.
(33) Kitayama, Y.; Nishiwaki-Ohkawa, T.; Sugisawa, Y.; Kondo, T. KaiC intersubunit communication facilitates robustness of circadian rhythms in cyanobacteria. *Nat Commun* **2013,** *4*, 2897.
(34) Chang, Y. G.; Cohen, S. E.; Phong, C.; Myers, W. K.; Kim, Y. I.; Tseng, R.; Lin, J.; Zhang, L.; Boyd, J. S.; Lee, Y.; et al. A protein fold switch joins the circadian oscillator to clock output in cyanobacteria. *Science* **2015,** *349*, 324-328.
(35) Murayama, Y.; Mukaiyama, A.; Imai, K.; Onoue, Y.; Tsunoda, A.; Nohara, A.; Ishida, T.; Maeda, Y.; Terauchi, K.; Kondo, T.; et al. Tracking and visualizing the circadian ticking of the cyanobacterial clock protein KaiC in solution. *EMBO J* **2011,** *30*, 68-78.
(36) Chang, Y. G.; Kuo, N. W.; Tseng, R.; LiWang, A. Flexibility of the C-terminal, or CII, ring of KaiC governs the rhythm of the circadian clock of cyanobacteria. *Proc Natl Acad Sci USA* **2011,** *108*, 14431-14436.
(37) Chang, Y. G.; Tseng, R.; Kuo, N. W.; LiWang, A. Rhythmic ring-ring stacking drives the circadian oscillator clockwise. *Proc Natl Acad Sci USA* **2012,** *109*, 16847-16851.
(38) Oyama, K.; Azai, C.; Nakamura, K.; Tanaka, S.; Terauchi, K. Conversion between two conformational states of KaiC is induced by ATP hydrolysis as a trigger for cyanobacterial circadian oscillation. *Sci Rep* **2016,** *6*, 32443.
(39) Hong, L.; Vani, B. P.; Thiede, E. H.; Rust, M. J.; Dinner, A. R. Molecular dynamics simulations of nucleotide release from the circadian clock protein KaiC reveal atomic-resolution functional insights. *Proc Natl Acad Sci USA* **2018**, doi: 10.1073/pnas.1812555115.
(40) Henzler-Wildman, K.; Kern, D. Dynamic personalities of proteins. *Nature* **2007**, *450*, 964-972.
(41) Mutoh, R.; Nishimura, A.; Yasui, S.; Onai, K.; Ishiura, M. The ATP-mediated regulation of KaiB-KaiC interaction in the cyanobacterial circadian clock. *PLoS One*

2013, *8*, e80200.

(42) Mukaiyama, A.; Furuike, Y.; Abe, J.; Yamashita, E.; Kondo, T.; Akiyama, S. Conformational rearrangements of the C1 ring in KaiC measure the timing of assembly with KaiB. *Sci Rep* **2018,** *8*, 8803.

(43) Nakajima, M.; Ito, H.; Kondo, T. In vitro regulation of circadian phosphorylation rhythm of cyanobacterial clock protein KaiC by KaiA and KaiB. *FEBS Lett* **2010,** *584*, 898-902.

(44) Nishiwaki, T.; Kondo, T. Circadian autodephosphorylation of cyanobacterial clock protein KaiC occurs via formation of ATP as intermediate. *J Biol Chem* **2012,** *287*, 18030–18035.

(45) Egli, M.; Mori, T.; Pattanayek, R.; Xu, Y.; Qin, X.; Johnson, C. H. Dephosphorylation of the core clock protein KaiC in the cyanobacterial KaiABC circadian oscillator proceeds via an ATP synthase mechanism. *Biochemistry* **2012**, *51*, 1547–1558.

(46) Rose, A. S.; Bradley, A. R.; Valasatava, Y.; Duarte, J. M.; Prlić, A.; Rose, P. W. NGL viewer: web-based molecular graphics for large complexes. *Bioinformatics*, **2018**, *34*, 3755–3758.

Supporting Information

Effects of Stochastic Single-Molecule Reactions on Coherent Ensemble Oscillations in the KaiABC Circadian Clock

Masaki Sasai
Department of Applied Physics, Nagoya University, Nagoya 464-8603, Japan

Supporting Text

In this supporting text, we explain Eqs. 2, 3, 6 and 7 of the main text. In our model, the binding status of molecular complexes in the system is represented by a set of $3N$ variables $\{i_{1k}, i_{2k}, j_k\}$ with $k = 1, \cdots, N$, where $0 \leq i_{1k} \leq 6$ is the number of KaiB molecules bound on the CI domains of kth KaiC hexamer, $i_{2k} = 0$ or 1 is the number of KaiA dimer bound on the CII ring of the kth KaiC hexamer, and $0 \leq j_k \leq i_{1k}$ is the number of KaiA dimers bound on KaiB in the kth KaiCB complex. Thus, by writing the probability that a binding status $\{i_{1k}, i_{2k}, j_k\}$ is realized in the system at time t as $P(i_{11}, i_{21}, j_1, \cdots, i_{1k}, i_{2k}, j_k, \cdots, i_{1N}, i_{2N}, j_N, t)$, the stochastic binding/unbinding reactions are described by a master equation for this probability. We approximate this N-body probability by factorizing it into one-body probabilities as

$$P(i_{11}, i_{21}, j_1, \cdots, i_{1k}, i_{2k}, j_k, \cdots, i_{1N}, i_{2N}, j_N, t) = \prod_{k=1}^{N} P(i_{1k}, i_{2k}, j_k, t). \qquad \text{(S1)}$$

This Hartree-like approximation was used to describe the single-molecular stochastic reactions in the system of gene expression.[1] We can further write $P(i_{1k} = 0, i_{2k} = 1, j_k, t) = P_{\mathrm{C_6A_2}}(k, t)$, $P(i_{1k} = 0, i_{2k} = 0, j_k, t) = P_{\mathrm{C_6B_0}}(k, t)$, and $P(i_{1k} = i, i_{2k} = 0, j_k = j, t) = P_{\mathrm{C_6B_iA_{2j}}}(k, t)$ assuming $P(i_{1k} \neq 0, i_{2k} \neq 0, j_k, t) = 0$. Because reactions in the CI domains and those in the CII domains are related only indirectly through the allosteric communication $W(k)$, we can separately write the master equations for $P_{\mathrm{C_6A_2}}(k, t)$ and $P_{\mathrm{C_6B_iA_{2j}}}(k, t)$. The equation for $P_{\mathrm{C_6A_2}}(k, t)$ is

$\frac{d}{dt}P_{\mathrm{C_6A_2}}(k,t) = h_A x P_{\mathrm{C_6B_0}}(k,t) - f_A P_{\mathrm{C_6A_2}}(k,t),$ which leads to Eq. 2 under the quasi-equilibrium approximation of KaiA binding/unbinding. With the same quasi-equilibrium approximation, KaiB binding/unbinding reactions are described without considering whether KaiA is bound on KaiB or not. Therefore, the master equations for $P_{\mathrm{C_6B}_i\mathrm{A}_{2j}}(k,t)$ are summarized by writing $P_{\mathrm{C_6B}_i}(k,t) = \sum_{j=0}^{i} P_{\mathrm{C_6B}_i\mathrm{A}_{2j}}(k,t)$, which leads to Eq. 3. We should note that $P_{\mathrm{C_6B_0}}(k,t)$ appearing in Eqs. 2, 3, and 5 relates $P_{\mathrm{C_6B}_i}$ and $P_{\mathrm{C_6A_2}}$.

For simplicity, we assume that KaiA dimer binds to and unbinds from every KaiB molecule without showing cooperative interactions between different KaiA dimers or between neighboring KaiB monomers on KaiC. Then, the ratio of the KaiA-bound KaiB to the KaiA-unbound KaiB should be $g_{BA}x = h_{BA}x/f_{BA}$. Therefore, if the number of KaiB molecules on the KaiC is i, the expected number of KaiA dimers bound in that KaiCBA complex is $i\, g_{BA}x/(1 + g_{BA}x)$. Then, the expectation value of the total number of KaiA dimers bound in KaiCBA complexes in the system should be

$$\frac{g_{BA}x}{1 + g_{BA}x} \sum_{k=1}^{N} \sum_{i=1}^{6} i P_{\mathrm{C_6B}_i}(k,t), \qquad \text{(S2)}$$

where $P_{\mathrm{C_6B}_i}(k,t)$ is the probability that i molecules of KaiB are bound on kth KaiC at time t. By dividing this factor with volume, we have the last term in Eq. 6.

For discussing the structure change of the kth KaiC hexamer, we assume that free energy F_k is affected by the level of phosphorylation U_k, probability of KaiA binding on the CII ring of KaiC hexamer p_k^{CA}, probability that KaiB binds to the CI domains of jth subunit of KaiC hexamer p_{kj}^{CB}, and the effect of ATP hydrolysis q_k as

$$F_k = -\frac{1}{6}\sum_{j=1}^{6} w_j(k)\,(c_0 - c_1 U_k + c_2 p_k^{CA} - q_k)$$

$$+c_3 \sum_{j=1}^{6} w_j(k)\, p_{kj}^{CB} - J \sum_{j=1}^{5} w_j(k) w_{j+1}(k), \qquad \text{(S3)}$$

where $w_j(k)$ is the structure order parameter of jth subunit of kth KaiC hexamer with $W(k) = (1/6)\sum_{j=1}^{6} w_j(k)$. $J > 0$ in Eq. S3 represents the cooperativity of structural transitions in neighboring subunits. We may regard $w_j(k)$ as an Ising spin and U_k, p_k^{CA}, q_k, and p_{kj}^{CB} as external fields applied to spins. In our previous publication, the Monte Carlo-type simulation of this "spin" system was performed with Hamiltonian similar to Eq. S3 for analyzing the single-molecular KaiC oscillation.[2] In the large J limit, the cooperativity is strong enough to have $w_j(k) = W(k)$. Then, Eq. S3 is effectively represented by

$$H_k = -W(k)(c_0 - c_1 U_k + c_2 p_k^{CA} - q_k) + c_3 W(k) \sum_{j=1}^{6} p_{kj}^{CB}. \qquad \text{(S4)}$$

By writing $p_k^{CB} = \sum_{j=1}^{6} p_{kj}^{CB}$ and $C_k = c_0 - c_1 U_k + c_2 p_k^{CA} - c_3 p_k^{CB} - q_k$, we have $H_k = -W(k) C_k$. The expectation value of $W(k)$ at temperature T should be

$$\langle W(k) \rangle = \sum_{W=-1}^{1} W \exp\left(-\frac{H_k}{k_B T}\right) \Bigg/ \sum_{W=-1}^{1} \exp\left(-\frac{H_k}{k_B T}\right) = \tanh\left(\frac{C_k}{k_B T}\right). \qquad \text{(S4)}$$

If we regard the quasi-equilibrium value $\langle W(k) \rangle$ as $W(k, t)$ in the slow dynamics, then we have Eq. 7.

References

1. Sasai, M; Wolynes, P. G. Stochastic gene expression as a many-body problem. *Proc Natl Acad Sci USA* **2003**, *100*, 2374–2379.
2. Das, S.; Terada, T. P.; Sasai, M. Single-molecular and ensemble-level oscillations of cyanobacterial circadian clock. *Biophys Physicobiol* **2018,** *15*, 136-150.